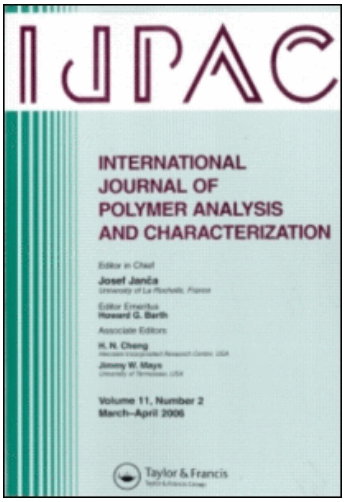

International Journal of Polymer Analysis and Characterization
Publication details, including instructions for authors and subscription information:
http://www.informaworld.com/smpp/title~content=t713646643

Scratch and Mar Performance of Coatings: Measurement and Structure Property Relationships

Karlis Adamsons[a]; Robert J. Barsotti[a]; Li Lin[a]; Basil V. Gregorovich[a]; Paul McGonigal[a]; Bruce Neff[b]; Greg Blackman[b]; Dave Nordstrom[c]
[a] Marshall Research Laboratory, DuPont Company, Philadelphia, PA, USA [b] Experimental Station Laboratory, DuPont Company, Wilmington, DE, USA [c] Troy Research Laboratory, DuPont Company, Troy, MI, USA

To cite this Article Adamsons, Karlis , Barsotti, Robert J. , Lin, Li , Gregorovich, Basil V. , McGonigal, Paul , Neff, Bruce , Blackman, Greg and Nordstrom, Dave(2000) 'Scratch and Mar Performance of Coatings: Measurement and Structure Property Relationships', International Journal of Polymer Analysis and Characterization, 5: 4, 289 — 311
To link to this Article: DOI: 10.1080/10236660008034629
URL: http://dx.doi.org/10.1080/10236660008034629

Int. J. Polym. Anal. Charact.,
2000 Vol. 5, pp. 289–311
Reprints available directly from the publisher
Photocopying permitted by license only

Scratch and Mar Performance of Coatings: Measurement and Structure Property Relationships

KARLIS ADAMSONS[a,*], ROBERT J. BARSOTTI[a], LI LIN[a], BASIL V. GREGOROVICH[a], PAUL McGONIGAL[a], BRUCE NEFF[a], GREG BLACKMAN[b] and DAVE NORDSTROM[c]

[a]*Marshall Research Laboratory, DuPont Company, 3401 Grays Ferry Ave., Philadelphia, PA 19146, USA;* [b]*Experimental Station Laboratory, DuPont Company, Route 141 & Henry Clay Ave., Wilmington, DE 19880, USA;* [c]*Troy Research Laboratory, DuPont Company, 945 Stephenson Hwy., Troy, MI 48007, USA*

(Received 23 October 1996; In final form 28 September 1998)

Scratch and mar of coatings is an important aspect of retaining initial performance levels. A number of test methods have been developed to measure coating resistance to damaging conditions. For the coatings industry, it is critical to have accelerated tests that indicate probable long term (i.e., service life) performance, and to have a means to correlate mar performance with chemical substructures of coatings. In this paper the synergism of measurement techniques for monitoring scratch and mar performance is explored. Laboratory mar tests, which have been validated by commercial experience, are used as the basis for comparison of a coating's performance. The combined elements of chemical, physical, mechanical, morphological and appearance properties of coatings have been explored. Chemical changes during cure and subsequent exposure have been followed by infrared techniques which show degree of cure, extent of photo-oxidation and hydrolysis, as well as changes in cross-linking with time and temperature. Physical and mechanical properties measured include T_g, hardness, standard stress/strain measurements, as well as "Method of Essential Work". Physical properties can be correlated with visual recovery of plastic flow damage and resistance to mar. Furthermore, micro-scratch experiments have been utilized to explore forces that are needed to induce surface damage and to determine the transitions between elastic deformation, plastic flow, and brittle fracture type damage. Morphology of scratches was examined by the use of atomic force microscopy before and after exposure. Optical imaging techniques were used to characterize scratch and mar. These studies are useful in understanding mechanisms of coating failure.

* Corresponding author.

Keywords: Scratch and mar resistance; "Method of Essential Work"; Microscratch testing; Cure analysis; Structure property relationships

INTRODUCTION

Most automobiles are coated with a basecoat/clearcoat coating system where the basecoat provides the color component and the clearcoat provides the high gloss and performance attributes. These systems offer exceptional initial appearance attributes. Increasing attention is being given to the ability of coatings to retain "new" car appearance by resisting weathering, chemical and physical damage, which includes scratch and mar.[1–6]

Scratch and mar damage has become a critical issue for Automotive Original Equipment Manufacturers (OEM).[7] One reason is that there are indications that the most significant contributor to such damage is carwashing, which is a normally required periodic activity. In addition, certain coatings have a problem with in-plant marring due to early sensitivity to mechanical damage after exiting the curing ovens. On weathering, coatings tend to lose some of their elasticity and thus scratch and mar performance tends to deteriorate. This change in performance is very dependent on the cross-linking chemistry and the polymer architecture. An additional factor that must be considered is the ability of coatings to recover after damage. From sun exposure, coatings can reach temperatures of up to 90°C. With some coatings this gives an opportunity to re-flow (i.e., heal) some or all of the plastic deformation damage that has occurred.

This study was conducted to gain a basic understanding of the fundamental film properties which affect scratch and mar performance. This understanding should help gain insight into the fundamental mechanisms involved in overall mar resistance, physical attributes that are needed for superior performance, and the chemical architecture and cross-linking needed to provide superior damage resistance.

EXPERIMENTAL

System Description

The systems were comprised of low-molecular-weight (6–10,000 M_w), hydroxyl functional, acrylic polymers cross-linked with an isocyanate

TABLE I Coating compositions used in "Method of Essential Work" study

Designation	*Composition as weight %*
A	100% A
B	80% A/20% F
C	60% A/40% F
D	40% A/60% F
E	20% A/80% F
F	100% F

oligomer (i.e., triisocyanurate of hexamethylene diisocyanate). The cure variations (high- and low-cure systems) were obtained by altering the catalyst. The types of catalyst used were typical for isocyanate-based systems (e.g., dibutyl tin dilaurate).

The films used in the "Method of Essential Work" included a proprietary rigid clearcoat (A), a proprietary flexible clearcoat (F), and blends of the two as indicated in Table I.

Film Preparation

The clearcoats were drawn down over either Uniprime electrocoat (ED-5000, PPG Industries, Pittsburgh, PA), thermoplastic olefin (TPO), or black waterborne basecoat using a 7 mil drawdown blade. The clearcoats were flashed (removing the majority of the volatiles) for 10 min at room temperature and then cured at 130°C for 30 min.

Clearcoat films for the "Method of Essential Work" study were prepared by spraying the formulations onto TPO panels which act as a release substrate.

Microhardness

The microhardness of the coatings was measured using a Fischerscope™ microhardness tester model HM100VS-B (Fischer Technology Inc., Ledgewood, NJ). The tester was set for a maximum force of 100 mN, ramped in a series of 50, 1 s steps. After the maximum force was attained, the tester relaxed the force in the same series of steps. The hardness was recorded in N/mm^2. This tester also gave data on percent elastic recovery (recovered depth/penetration depth), total work, percent elastic work, and percent plastic work.

Swell Ratio

The swell ratio of the free films (removed from TPO) was determined by swelling in methylene chloride. The free film was placed between two layers of aluminum foil and a disc of about 3.5 mm diameter was punched out of the film. The aluminum foil was removed from either side of the free film. Using a microscope with 10× magnification and a filar (i.e., scaled) lens, we measured the unswollen diameter (D_0) of the film. Four drops of methylene chloride were added to the film. The film was allowed to swell for a few seconds and then a glass slide was placed over it. The swell ratio was calculated as:

$$\text{swell ratio} = (D_s)^2/(D_0)^2.$$

Mar Testing

Scratch and mar damage to coatings can be categorized broadly as dry or wet (lubricated) mar. Wet mar, for example, occurs in car washing, which generally is considered the most significant contributor to scratch and mar damage, and in buffing operations used during repair. Dry mar comes from a broad range of materials that can contact the coating such as clothing, paper, building materials, blowing sand, bushes, etc. It is important to note that coatings do not necessarily respond in the same way to these conditions. It is not unusual to have systems that are good in wet mar but poor in dry mar, and vice versa. There are a number of reasons for this. One specific case includes systems with a high coefficient of friction that typically show poor dry mar performance, but may have excellent wet mar performance because lubrication often lowers the friction effect. For this reason, we recommend that both a dry test and a wet test be performed. Figure 1 illustrates the methods commonly used to apply mar damage.

After conducting the mar test on a coating and evaluating the resultant mar, the coatings were heated for 1 h above their T_g (70°C was used in this study) and the mar was re-evaluated. This allowed for mar recovery and for differentiation between non-recoverable, permanent, brittle fracture and potentially recoverable plastic flow damage. This is referred to as heat-recovered mar. In addition, panels stored at room

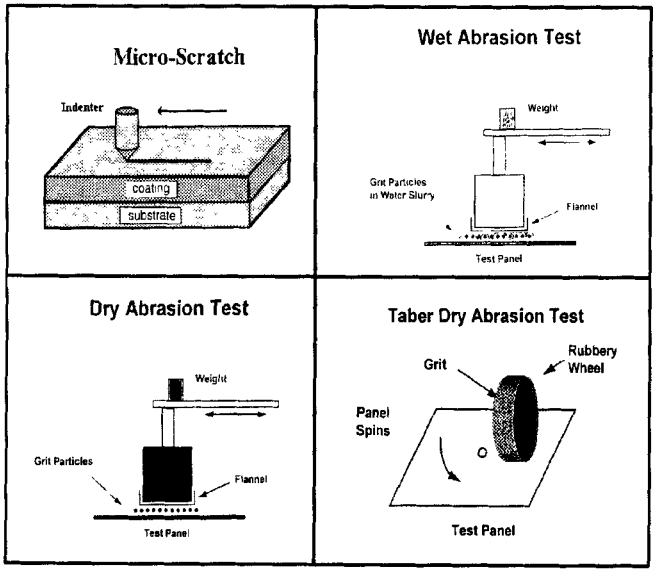

FIGURE 1 Mar damage methods: the nano-indenter microscratch, wet abrasion, dry abrasion and Taber (dry) abrasion tests.

temperature were re-evaluated for mar after 7 days. This is referred to as room-temperature-recovered mar.

Wet Mar Marring is accomplished using a test device that has a reciprocating motion with either the arm or the panel moving. The arm is equipped with a block to which a felt pad is mounted. The surface of a test panel is marred using a slurry of aluminum oxide in water and a felt pad. Critical variables include the felt pad, grit size, grit concentration, weight, and number of cycles. The choice of felt material is critical. It is best to find material that itself does not scratch the surface. All of the damage is assumed to come from the grit slurry. Materials used in metallurgical polishing have been found to be useful. For automotive clearcoats, useful standard conditions are 500 g, 10 cycles, 320-grit aluminum oxide at a concentration of 0.1%. The Gakushin type Rub Tester Model NR-100 (Daiei Kagaku Seiku Mfg. Co. Ltd., Kyoto, Japan) has been found to be particularly useful for performing this test. The ratings shown were obtained by optical imaging that had been calibrated to match human perception. On the scale used, 100 represents an unmarred coating.

Dry Mar The same Daiei tester can also be used to perform the dry test. In this test, a cleansing powder was sprinkled on the surface of a panel, the excess was tapped off and the panel placed in the Daiei Rub Tester with a dry felt pad placed on the mounting block. For automotive clearcoats useful conditions are Bon-Ami™ Powder (Faultless Starch, Bon Ami Co., Kansas City, MO), 15 cycles with a weight of 700 g. The ratings were determined by image analysis in the same fashion as wet mar.

Crock Test The AATCC Crock meter Model CM-5 (Atlas Electric Devices Co., Chicago, IL) could also be used to perform the dry test. The test was performed as described above with 10 cycles normally used. The percent gloss retention of the damaged vs. undamaged areas were recorded.

Taber Mar A different dry test was performed on the Taber Abraser™ Model 503 (Taber Instruments, North Tonawanda, NY). This is a very aggressive test and since the grit cannot roll, this test appears to relate best to stylus type damage, such as from a sharp object. In this instrument, a panel with a hole drilled in the middle was placed on the spindle of the test device. A rubbery wheel, in which an abrasive is imbedded, was placed on the panel. In most configurations there are two wheels. The panel was rotated to inflict the mar damage on the test coating. Useful conditions for automotive clearcoats were a CS-10 wheel, 500 g and 10 cycles. Rating was determined by percent gloss retention or optical imaging.

Single Indentor Microscratch Test

To understand the mechanism of mar damage, we have developed the microscratch technique to quantitatively study scratch and mar behavior of coatings. The detailed experiments and apparatus are presented elsewhere.[8] In a typical microscratch experiment, a well-defined indenter is controlled to penetrate into a coating surface while the coating is moved perpendicular to the penetration motion. During this process, indentor displacement (nm) normal and tangential forces (μN) required to cause scratch type damage were continuously measured, and the damage event was recorded by use of a microscope equipped with a video camera. The controllable parameters of a

microscratch experiment are penetration rate, scratch rate, lubrication condition, cutting geometry, and coating temperature.

In the current application, a ramp function was used to vary the indentor displacement. Figure 2 shows the output from a typical microscratch experiment. It shows a plot of penetration depth, normal force (N), and tangential force (T) as a function of scratch distance on a cross-linked clearcoat surface. As illustrated, the normal force curve and tangential force curve change from a smooth increase with penetration depth to rapid oscillation and chatter. With video microscopy, changes in deformation mode progressing from elastic to plastic, and then to fracture, have been observed as the indentor penetrated further into the coating. Atomic force microscopy (AFM) imaging was used to follow changes in the deformation mode. The changes from a smooth curve increasing to chatter of the normal and tangential force curves were a response to the deformation mode transition from plastic plowing to fracture where damage was uneven and considerably more severe. Microscratch experiments performed under ramping function control caused coatings to undergo elastic deformation to visco-plastic plowing and then to fracture. The critical mechanical thresholds of the

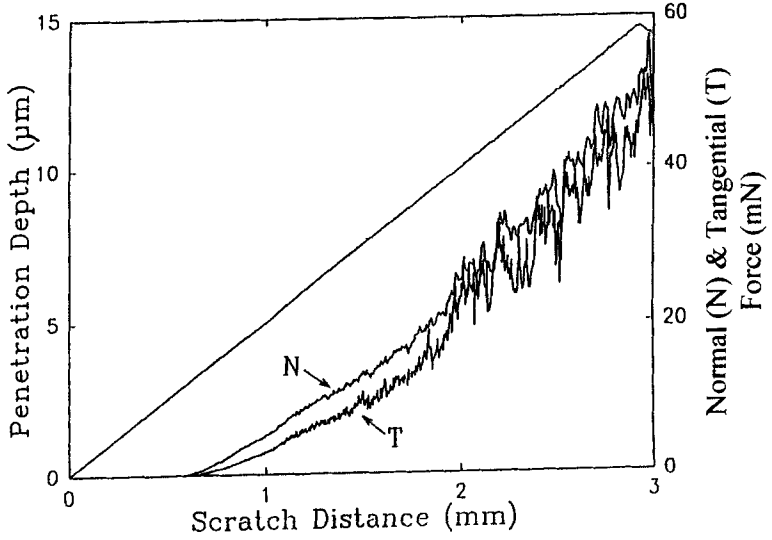

FIGURE 2 Microscratch analysis of acrylic/melamine clearcoat; plot of penetration depth (μm), normal (N) and tangential (T) force vs. scratch distance (mm).

transitions could be identified with precision. These physical quantities are necessary for a more complete understanding of mar behavior of coatings. In addition, work is under way to correlate onset and changes in deformation mode with visual (optical) perception of type and degree of coating damage. Of particular interest are ongoing efforts to correlate the measurable onset of mechanical damage with our visual perception of damage.

Atomic Force Microscopy (AFM)

The principle of operation of the AFM is similar to that of a stylus profilometer, except that the probe is very sharp (< 100 Å radius) and the forces are in the nano-Newton range. The probe is attached to a microfabricated cantilever which bends under the influence of surface forces. In "normal" or contact mode of imaging the probe is brought to within atomic dimensions of the surface under piezoelectric control. The cantilever bends in response to the surface forces and the minute deflections are measured using a focused laser reflected off the back of the cantilever. Images are obtained by scanning the tip via piezoelectric transducers and measuring the response of the cantilever at each point. The resolution of the AFM that was used (Model Autoprobe M5, Park Scientific Instruments, Sunnyvale, CA) is < 1 nm.

A considerable advantage of the AFM is that height and surface roughness information is obtained directly from the images. Lateral and height calibrations are checked prior to each experiment by imaging a NIST traceable standard from VLSI Standards Incorporated, Surface Topography Standard, Model STS-440. A variety of statistical descriptions of the surface are available using commercial software (e.g., RMS roughness, average roughness, etc.). Also, data analysis algorithms specific to scratch and mar have been developed in-house for the single indenter microscratch test application.

Optical Imaging

Scratch and mar damage inflicted by the rub test methods were evaluated by an optical imaging protocol based on the commercially available Bioscan Optimus system (Optimus Corporation, Seattle, WA). For dense scratch damage of this type, it was found suitable to use a

pixel count method whereby each scratch appears as a light streak and the damage was assessed by the number of pixels at each level of brightness. A gray scale (0–255) histogram was obtained. The histogram was scaled to human perception (average visual observation) by a curve fit formula.[9] The scale obtained runs from "0" at the poorest extreme to "100" which indicates no damage.

Cure Analysis by Infrared

Chemical changes during cure and subsequent exposure have been followed by time-lapse infrared techniques which show extent of photo-oxidation and hydrolysis, as well as changes in cross-linking density, with time and temperature.[10] The cure condition of a coating was monitored by infrared (IR) transmission mode analysis. Free films, material skived from the surface of coated panels, and silicon wafers with a thin layer (~ 2–$3\,\mu m$ thick) of coating, were evaluated for changes in chemical functionality versus time/temperature. Free films and skived surface material were analyzed using a Nicolet FT-IR Spectrophotometer Model 20-SXC (Nicolet Instrument Corporation, Madison, WI) equipped with a SpectraTech IR-Plan™ (Spectra-Tech Incorporated, Stamford, CT) microscope. The coated silicon wafers were analyzed with the same FT-IR, standard sample compartment.

For isocyanate-derived coatings the disappearance of the NCO peak (~ 2270–$2280\,cm^{-1}$) was followed to monitor the extent of cure and associated kinetics. IR spectra were obtained prior to cure (bake), immediately after bake at 265°F, 7 days after bake, and 30 days after bake.

Glass-Transition Temperature (T_g)

The glass-transition temperature of the film was determined using differential scanning calorimetry, TA Instruments Model 2920 DSC (TA Instruments Incorporated, New Castle, DE).

Tensile Properties

The tensile properties were run using free films on an electro-mechanical tensile test machine Model 1123 (Instron Corporation, Canton, MA)

and pulled until rupture occurs. The test speed used on most of the films was 5 mm/min. On the low hardness, well-cured system a speed of 2 mm/min was used.

Method of Essential Work

The "Method of Essential Work" is based on Broberg's separation of the nonelastic region around the crack tip into an inner zone in which fracture occurs and an outer zone of plastic deformation.[11,12] An excellent discussion of the "Method of Essential Work" and its application has recently been given by Chan and Williams[13] who also point out the inapplicability of other fracture mechanics methods to thin-film situations. The technique of the "Method of Essential Work" is simply described; however, in practice great care must be taken to ensure reproducible results.[14]

Thin strips of clearcoat formulations were obtained from spray-outs onto a release substrate such as TPO; a width of 1 in was found to be satisfactory. Equal and opposite notches were cut into the strips with new razor blades to yield ligaments of different lengths subject to the criteria that the longest ligament was not greater than 1/3 of the sample width and the shortest ligament greater than three times the sample thickness. With care such samples can be readily inserted into the jaws of an Instron tensile test machine and pulled until rupture occurs. Data were recorded as pairs of energy to break values (in this case total work of fracture, W_f) and ligament lengths.

W_f versus L gives a straight line represented as $W_f = W_e + W_p L$ in which W_e, the intercept, is the essential work of fracture and W_p, the slope, is the work of plastic deformation. Convenient units for W_f and W_e are kJ/m^2, and kJ/m^3 for W_p. The quality intuitively regarded as toughness is associated with elevated values of both W_e and W_p.

Scanning Electron Microscopy (SEM)

Scanning electron microscopy was done using a Philips SEM Model 505 (Philips Electronics, Einhoven, Netherlands) equipped with a Tracor Northern Series EDXRF system (Noran Corporation, formerly Tracor Northern, Middleton, WI). SEM was used to monitor the morphology of coatings at magnifications from 500–1500.

RESULTS AND DISCUSSION

Testing

Extensive testing was conducted on the clearcoats: initially (on the same day as oven curing at 130°C), one day later, ~1 week later, and ~1 month later. Testing included: (1) mar testing: Taber, wet and dry mar testing with damage evaluated by optical image analysis immediately after mar damage, after recovering at room temperature for 7 days, and after the marred clearcoat was heated for 1 h @ 70°C; (2) microscratch testing: using a single indentor microscratch test developed in-house,[8] (3) cure testing: including hardness (Fischer), swell ratio and infrared analysis; (4) tensile properties; (5) glass-transition temperature; (6) scanning electron microscopy; and (7) atomic force microscopy.

Infrared Cure

Infrared spectra for the low- and high-cure systems were obtained. The initial bake spectra for low-cure and high-cure systems are shown in Figure 3A and B, respectively. Table II shows the change in residual isocyanate concentration in these systems as a function of bake and room temperature aging. The peak at approximately 2280 cm^{-1} is attributed to the isocyanate (NCO) functional group absorption. The absorption of styrene @ 710 cm^{-1} is used as an internal reference.

There is a major difference in the residual isocyanate in the low-cure system vs. the high-cure system. As mentioned above, these systems are equivalent in composition, the difference in residual isocyanate indicates a lower extent of cure in the low-cure system. Upon room temperature aging, the residual isocyanate levels become similar for both low- and high-cure systems.

Swell Ratio

The swell ratio (using methylene chloride as swelling solvent) of the low- and high-cure systems vs. room temperature aging is given in Table II. Initially, the swell ratio of the low-cure system is much higher than the high-cure system. This again indicates incomplete network formation. Upon aging, both films are similar.

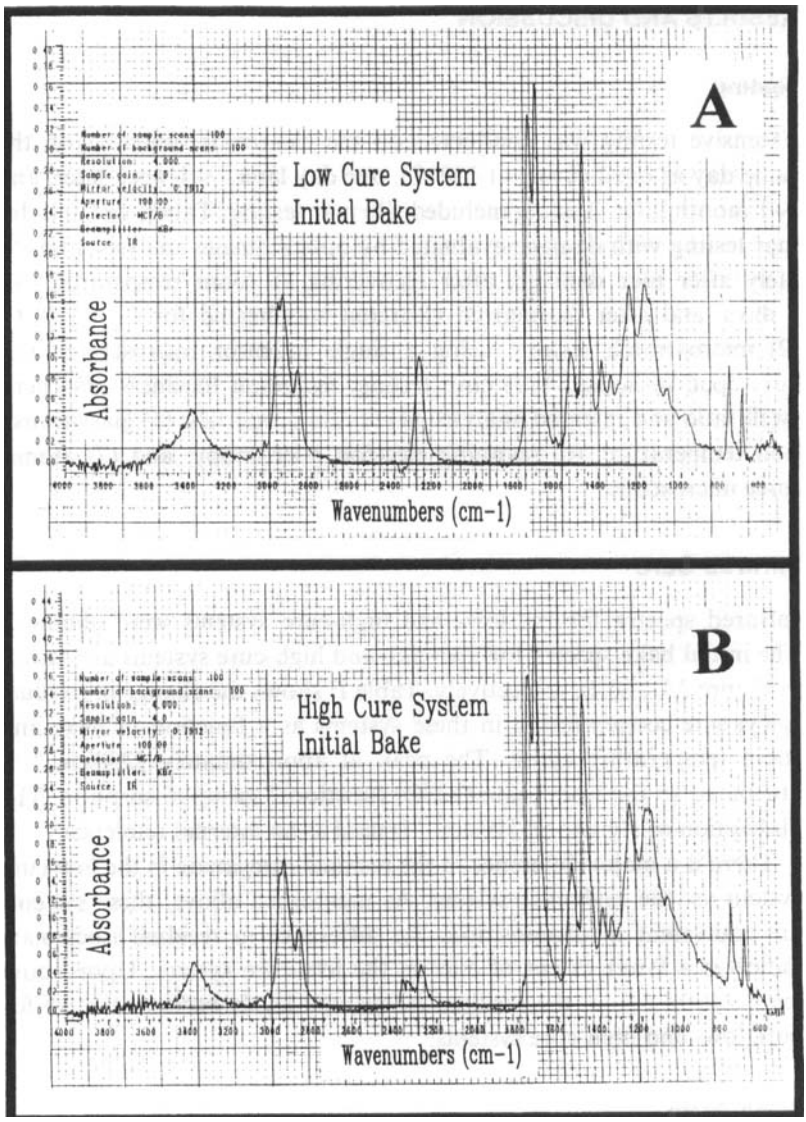

FIGURE 3 IR spectra for initial bake of low-cure (A) and high-cure (B) systems. Note the difference in isocyanate content @ 2250 cm^{-1}.

TABLE II Change in cure properties with time

	IR Peak ratio NCO/Styrene	*Swell ratio*	*Hardness* (N/mm^2)	*% Elastic recovery*
Initial				
Low cure	1.43	1.77	56	17
High cure	0.45	1.55	127	32
7 Day				
Low cure	0.77	1.56	110	37
High cure	0.33	1.55	129	38
30 Day				
Low cure	0.38	1.56	130	42
High cure	0.17	1.58	130	43

Hardness Development

The hardness and elasticity data given in Table II show that the low-cure system is softer and has a lower percent of elastic recovery. In this system, the network is not fully developed and, thus, the hardness and elastic recovery are lower. Upon aging, the hardness/elastic recovery become similar.

The cure data do confirm the initially lower extent of cure in the low-cure system versus the high-cure system. Upon room temperature aging, however, the systems become similar. This slow change at room temperature in the low-cure systems allows us to investigate the change in mar properties and other key film properties to obtain a better understanding of the mechanisms associated with mar resistance.

Mar Testing

The mar results in Figures 4–6 show: (1) Initially, the low-cure system was very poor for dry mar versus the high-cure system. The dry-mar values were low and they did not recover upon heating the film to 70°C. (2) Initially, the low-cure system showed better wet mar than the high-cure system but both recovered to the same value upon heating. (3) The Taber mar results were equivalent. The low-cure system did show better room temperature recovery (due to lower T_g). After the panels aged at ambient conditions (25°C/50% RH) for 7 days, the systems were essentially equivalent for mar.

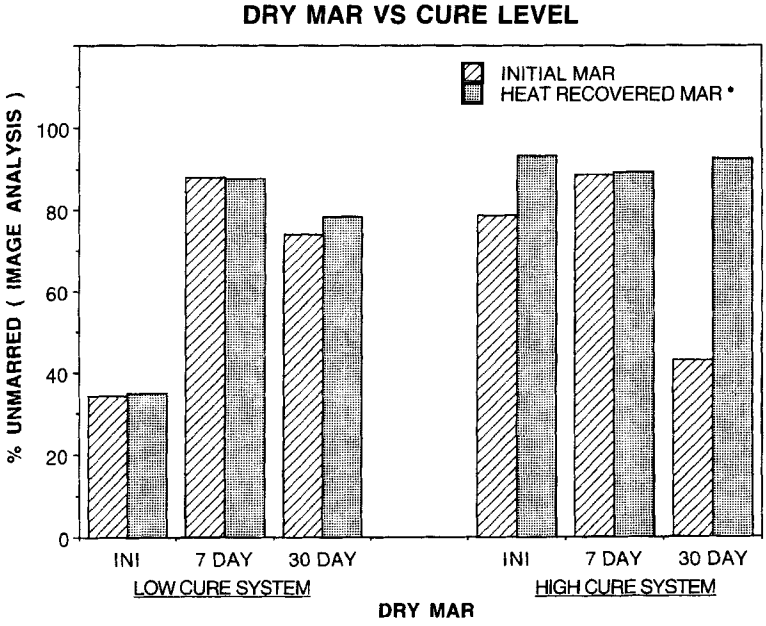

FIGURE 4 Analysis of dry mar vs. cure level. Plot of percent unmarred surface (as determined by image analysis) vs. time (days at room temperature) for a low-cure system and a high-cure system.

SEM Imaging

SEM imaging has been used to characterize the type of failure resulting from scratch and mar damage.[14] The SEM pictures in Figure 7 show the importance of characterizing the type of mar failure as well as the extent of failure, for plastic flow mar damage and brittle fracture mar damage, respectively. The images shown exhibit similar mar testing results (initially) but obviously via different mechanisms of failure. Upon heating above T_g, the plastic flow damage is recoverable; the brittle fracture damage is not.

Microscratch Data

Table III shows the critical coefficient of friction (coefficient of friction at fracture) and the critical normal and tangential load at fracture. This is shown initially and after room temperature aging. Figure 8

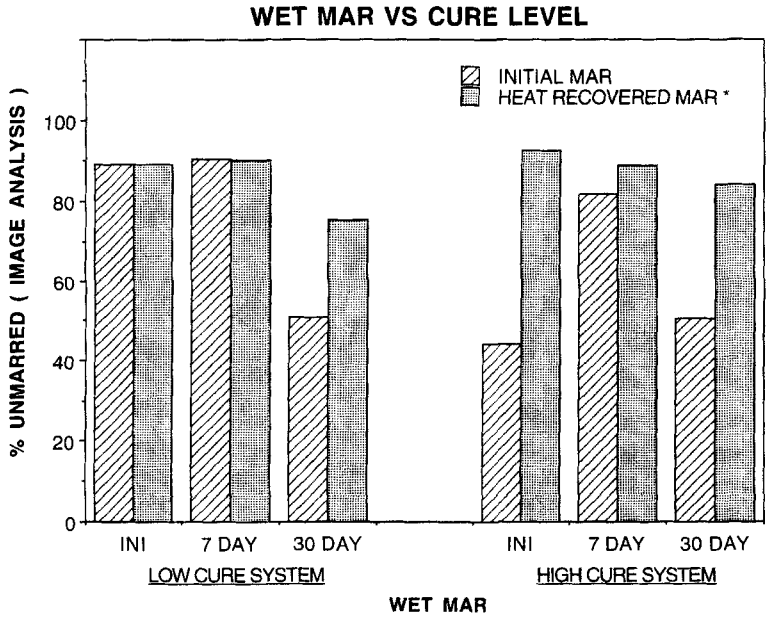

FIGURE 5 Analysis of wet mar vs. cure level. Plot of percent unmarred surface (as determined by image analysis) vs. time (days at room temperature) for a low-cure system and a high-cure system.

shows various plots of a low-cure system aged 7 days, including coefficient of friction, normal force, and tangential force vs. scratch distance.

Initially, the low-cure system fractures at a lower normal and tangential load vs. the high-cure system and is thus more susceptible to fracture under equivalent loads. The low-cure system initially shows a higher coefficient of friction and a lower force to fracture. The result is that, in the low-cure system, more of the marring normal force is transformed into tangential force across the surface of the panel being marred. This will result in more damage and should play a larger role in dry rub vs. wet rub where a lubricant (water) was used to reduce friction.

The Taber mar, although it is a dry test, appeared to be less affected by coefficient of friction in these tests. In the Taber test, the abrading material is embedded in the Taber wheel and is not free flowing as in the dry mar test, where material can roll around the surface of the

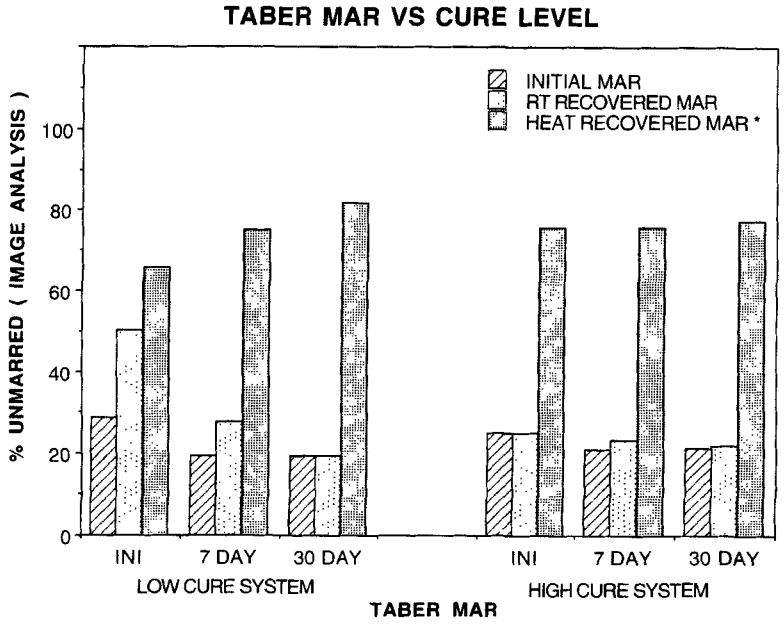

FIGURE 6 Analysis of Taber mar vs. cure level. Plot of percent unmarred surface (as determined by image analysis) vs. time (days at room temperature) for a low-cure system and a high-cure system.

panel and cause deep gouges in the film. This embedding can somewhat reduce differences in friction. Upon aging, the microscratch data for the films became similar.

Tensile Properties

The comparisons of tensile properties in Figures 9 and 10 showed that initially, the low-cure system exhibited a very low elastic limit vs. the high-cure system. This low elastic limit resulted in films which deformed more easily under marring conditions and which were less mar resistant. Upon aging, the tensile properties became similar.

For comparison, the tensile properties of a well-cured, low-hardness system are shown in Figure 11. This system exhibited excellent mar resistance. The tensile properties of this system showed no elastic limit. This is consistent with the above findings and shows that hardness alone is not indicative of mar resistance.

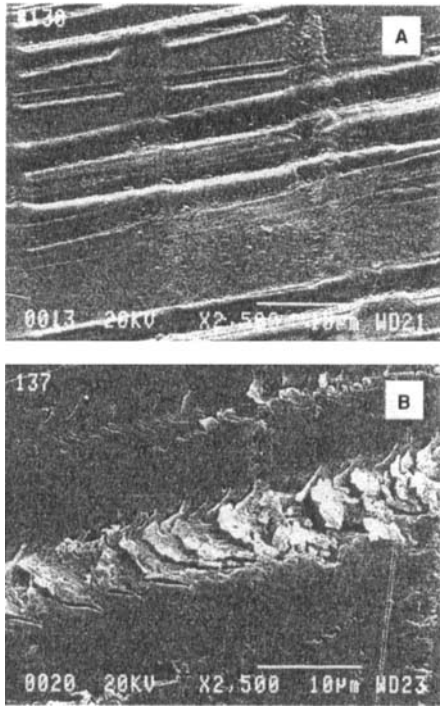

FIGURE 7 SEM microphotographs of (A) typical plastic flow mar damage on the surface of a clearcoat and (B) typical brittle fracture mar damage on the surface of a clearcoat.

TABLE III Changes in mechanical properties with time

	Critical coefficient of friction	*Critical normal load* (mN)	*Critical tangential load* (mN)
Initial			
Low cure	0.90	9.62	8.69
High cure	0.76	12.29	9.40
1 Day			
Low cure	0.83	9.04	7.46
High cure	0.75	12.61	9.46
7 Days			
Low cure	0.74	12.05	8.89
High cure	0.73	12.44	9.05

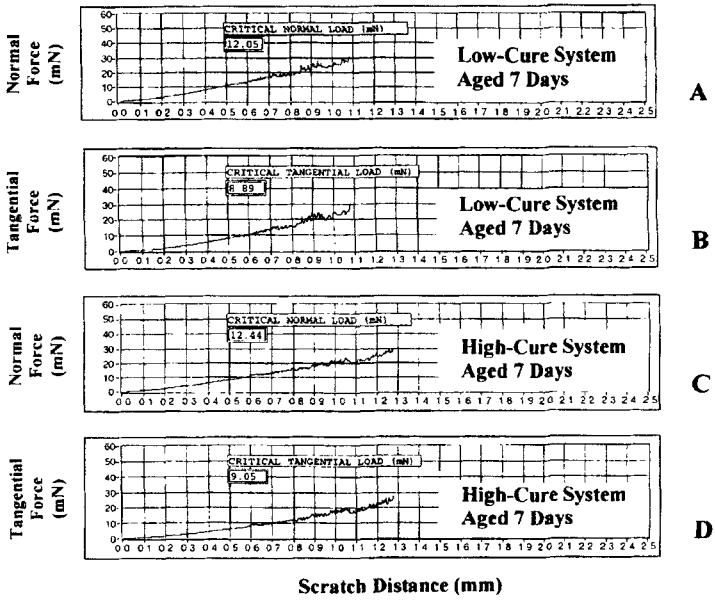

FIGURE 8 Plots of microscratch data at low-cure coating aged 7 days: (A) normal force vs. scratch distance; (B) tangential force vs. scratch distance; and of a high-cure coating aged 7 days: (C) normal force vs. scratch distance; (D) tangential force vs. scratch distance.

Glass-Transition Temperature

The T_g (DSC) data for a low-cure system are 25°C initially, 40°C after 7 days, and 48°C after 32 days. The T_g (DSC) data for a high-cure system are 43°C initially, 48°C after 7 days, and 48°C after 32 days. These results indicate that the low-cure system had a lower initial T_g, but on aging the films reached the same final T_g. The lower initial T_g (25°C) of the low-cure system allowed for more room temperature recovery of the less severe wet mar. This led to better initial wet mar for the low-cure system. The heat-recovered wet mar was equivalent for both systems (the recovery temperature used was above the T_g of both films).

"Method of Essential Work"

A "Method of Essential Work" study was conducted with a proprietary rigid clearcoat, a proprietary flexible clearcoat, and blends of the

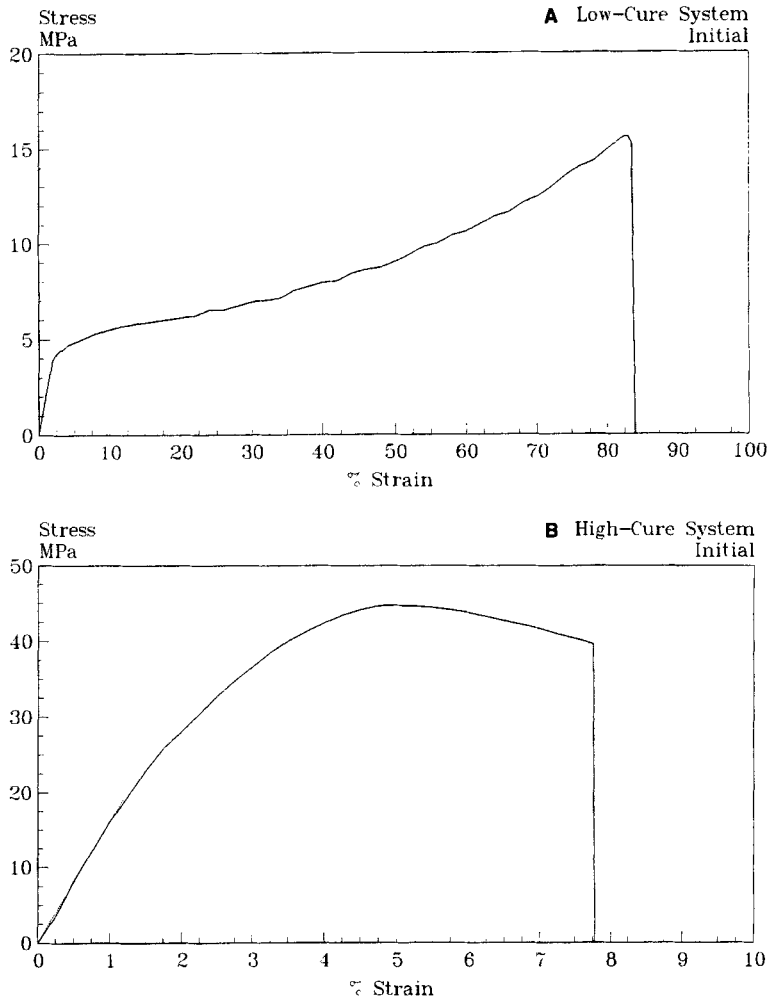

FIGURE 9 Plot of initial stress vs. strain curve for: (A) low-cure coating and (B) high-cure coating.

two (Table I). Attempts to correlate visual mar results (ranking) for the systems examined (A–F in Table I) with the ordinary tensile properties of stress, strain, modulus and energy to break were unsuccessful. However, application of the "Method of Essential Work" did yield the correct ranking of the systems in terms of the essential work of fracture (Table IV). Since marring affects only the outermost region of a very

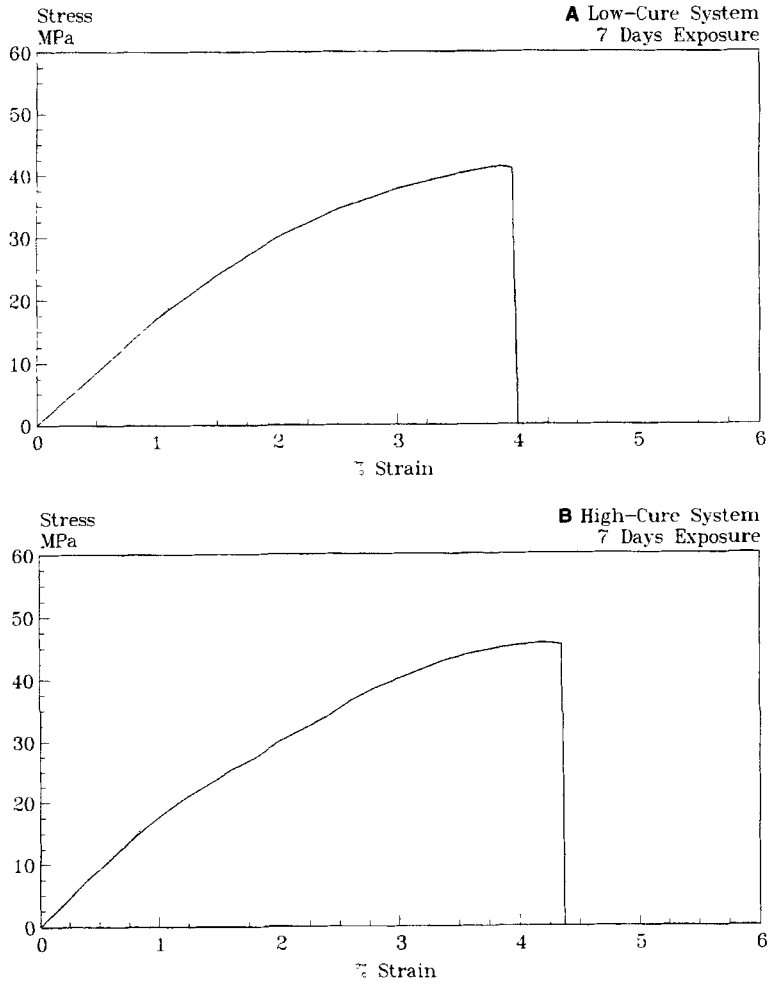

FIGURE 10 Plot of stress vs. strain curve after 7 days for: (A) low-cure coating and (B) high-cure coating.

thin film, plane stress fracture properties should be applicable, and directly correlate to results from the method of essential work. Unexpectedly, the best mar resistance was not shown by the flexible clear-coat F, but by E, the 20% A/80% F blend. This ranking is also given by the "Method of Essential Work".

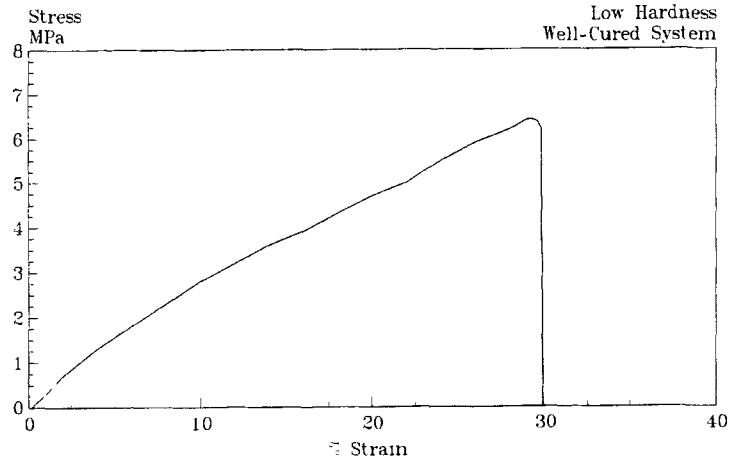

FIGURE 11 Plot of stress vs. strain curve of low-hardness, well-cured coating.

TABLE IV Method of essential work for flex/rigid systems. Systems range from rigid clearcoat A to flex clearcoat F. Systems B to E are blends of A and F. Mar rank was determined by visual ranking

System	*Mar rank*	*Peak strain %*	*Essential work of fracture* (kJ/m^2)
E	1	27.0	2.34
F	2	33.3	1.89
D	3	19.2	1.62
C	4	12.7	1.53
B	5	10.7	0.61
A	6	7.7	Brittle

SUMMARY AND CONCLUSIONS

From this work, general conclusions on mar resistance can be made. A need for accurate characterization of the mar behavior of a coating has been demonstrated. This includes the type of mar failure (elastic deformation, plastic flow damage, and brittle fracture), the degree of failure, and the recoverability of the mar damage. The critical factors influencing mar appear to be:

- Elastic limit or yield point: At higher values coatings have an improved ability to resist deformation under marring conditions.

- Extent of cure: The extent of cure can affect mar resistance. Properly cured systems will generally exhibit better mar performance. IR analysis provided a convenient and reproducible means of monitoring both bake and room temperature cure.
- Elastic recovery: A fully developed network with good elastic recovery is necessary to maximize the potential for immediate or time/temperature dependent mar recovery.
- Critical normal and tangential load: These values need to be maximized to avoid film fracture under application of low forces.
- Critical coefficient of friction at fracture: This value needs to be minimized so that less of the force applied during coating marring is in the tangential direction.
- T_g of the system appears to affect the recoverability conditions (time and temperature), but not the ability to recover. Lower T_g systems will show less mar, provided the tensile properties are reasonable.
- "Method of Essential Work": Visual mar resistance for a series of clearcoats ranging from rigid to flexible matched the "Essential Work of Fracture" ranking. However, these results did not correlate with tensile properties of stress, strain, modulus or energy-to-break.
- The wet mar test, using an aluminum oxide slurry for abrasion, and optical imaging for analysis, has been developed as an abrasion test that correlated well with commercial carwash data.
- Optical imaging: When scaled to human visual observations, optical imaging has been developed as the method of choice for quantifying mar data.
- Atomic force microscopy is a particularly useful method of examining mar damage to aid in determining mechanical failure mechanisms and damage characteristics resulting from the various marring procedures.
- A state-of-the-art microscratch single indenter technique provides a means of obtaining quantitative information on coating mechanical response to surface forces, and on transitions in response from elastic recovery, to visco-plastic deformation, and (eventually) to brittle fracture.

Acknowledgments

The authors would like to acknowledge Joanne Paci for mar image analyses and "Method of Essential Work" determinations, James

Halpin for IR analyses, Joseph Turrisi for DSC (T_g) analyses, and Sue Riggs for atomic force microscopy.

References

[1] R.A. Dickie, *J. Coat. Technol.*, **66**, 29 (1994).
[2] D.R. Bauer, *J. Coat. Technol.*, **66**, 57 (1994).
[3] D.R. Bauer, *Prog. Org. Coat.*, **14**, 193 (1986).
[4] J.W. Martin, S.C. Saunders, F.L. Floyd and J.P. Wineburg, NIST Building Science Series 172, *Methodologies for Predicting the Service Lives of Coatings Systems*, Building & Fire Research Lab, National Institute of Standards and Technology, 1994.
[5] R.A. Dickie, *J. Coat. Technol.*, **64**, 61 (1992).
[6] J.L. Gerlock, C.A. Smith, E.M. Nunez, V.A. Cooper, P. Liscombe and D.R. Cummings, Advances in Coating Technology: Predicting the Durability of Coatings, *Proceedings of the 36th Annual Technical Symposium*, Cleveland, OH, May 18, 1993.
[7] J.L. Courter, presented at the *23rd Annual International Waterborne, High-Solids and Powder Coatings Symposium*, February 14–16, 1996, New Orleans, LA
[8] L. Lin, G. Blackman and R.R. Matheson, *ACS Polym. Prep.*, **39**(2), 1218, 1998.
[9] B.V. Gregorovich and P.J. McGonigal, presented at *Finishing '93*, October 25–28, 1993, Cincinnati, OH.
[10] J.H. Hartshorn, *Application of FT-IR to Paint Analysis*, Analysis of paints and related materials: Current Techniques for Solving Coatings Problems, ASTM STP 1119, American Society for Testing and Materials, Philadelphia, 1992, pp. 127–147.
[11] K.B. Broberg, *J. Mech. Phys. Solids*, **19**, 407 (1971).
[12] K.B. Broberg, *J. Mech. Phys. Solids*, **23**, 215 (1975).
[13] W.Y.F. Chan and J.G. Williams, *Polymer*, **35**, 1666 (1994).
[14] B.V. Gregorovich and I. Hazan, *Prog. Org. Coat.*, **24**, 131 (1994).